

Observation of a New Thermoelectric Effect in Superconducting Thin Films

Hu Jong Lee, D. A. Rudman,^(a) and J. C. Garland

Department of Physics, Ohio State University, Columbus, Ohio 43210

(Received 14 September 1984)

Measurements are reported of a new thermoelectric effect in thin indium-indium-oxide superconducting films. In the temperature regime between the Kosterlitz-Thouless vortex dissociation temperature T_c and the BCS transition temperature T_{c0} , a simultaneous electric field and temperature gradient cause the film to become weakly magnetized with a magnetization normal to the plane of the film. The magnetization rises to a maximum between T_c and T_{c0} and is linear in both the temperature gradient and electric field.

PACS numbers: 74.40.+k, 74.50.+r

In this Letter, we report the observation of a new thermoelectric effect in superconducting thin films of high normal-state sheet resistance. This effect occurs over a narrow temperature range, bounded from above by the BCS transition temperature T_{c0} , and from below by the Kosterlitz-Thouless vortex-unbinding temperature, T_c .¹⁻⁵ The effect is created by the simultaneous application of an electric field and temperature gradient and is manifest as a spontaneous weak magnetization normal to the plane of the film. Our measurements generally support a recent proposal by Garland and VanHarlingen (GV)⁶ that thermoelectric fields break the symmetry of the distribution of unbound vortices in the Kosterlitz-Thouless regime, leading to a predominance of vortices of one polarity. This imbalance in the free vortex-antivortex population appears to be responsible for the observed magnetization in our experiments.

The samples in this study consist of high sheet resistance indium-indium-oxide (In/InO_x) composite films (8×22 mm²) on optically polished sapphire substrates. The films are prepared by reactive ion-beam sputtering,⁷ by use of a deposition rate of about 3 Å/sec and a rotating specimen holder to increase homogeneity. Typical film thicknesses are 100–300 Å (see Table I for additional sample information).

The sample configuration is illustrated schematically in Fig. 1, which shows the placement of electrodes, thermometers, and heaters. One end of the sapphire

substrate is thermally anchored to a liquid ⁴He pot, leaving the free end suspended in a vacuum. A temperature gradient ∇T transverse to the long dimension of the film is established by controlling both the ⁴He pressure in the pot and the current to two 2000-Å Si-Ta alloy film heaters deposited one on each end of the substrate. Two carbon film thermometers, 0.5 mm wide by 1 μm thick, are bonded directly to the substrate just inside the two heaters and are calibrated against a germanium resistance standard at the beginning of each run. The thermal conductance of the sapphire substrate is high enough that the thermometers and resistive In/InO_x film do not perturb significantly the temperature gradient along the substrate.

A dc electric field E is applied along the length of the film by injecting a dc current I into superconducting Pb electrodes (1500 Å thick) sputtered onto the ends of the In/InO_x film. The level of current I is kept low enough (typically 0.1–10 μA) to prevent substantial current-induced vortex depairing for the temperature range of interest. The primary winding of a superconducting flux transformer, placed directly over the film, couples the magnetic response of the sample to a SQUID magnetometer. The 1.1-μH primary coil consists of five turns of No. 50 niobium wire wound into a 6×10-mm² rectangular shape.

All measurements were carried out in a screened room. In addition, the entire cryostat was vibration isolated and surrounded by a double Mumetal shield.

TABLE I. $P(O_2)$ is the oxygen partial pressure during deposition, t is the film thickness, $\rho(300)$ is the room-temperature resistivity, and R_n is the normal-state sheet resistance.

Sample	$P(O_2)$ (mTorr)	t (Å)	$\rho(300)$ (mΩ cm)	R_n^{\square} (Ω/□)	T_c (K)	T_{c0} (K)
1	0.09	120	1.70	1590	3.105	3.286
2	0.15	250	1.79	945	2.942	3.055
3	0.18	250	2.00	1115	2.705	2.843
4	0.13	150	1.71	1530	3.122	3.298

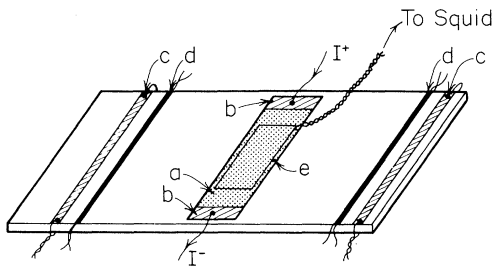


FIG. 1. Details of sample construction: (a) In/InO_x film, (b) current electrodes, (c) heaters, (d) thermometers, (e) flux-transformer primary coil.

It was found necessary to keep the residual magnetic field below 0.5 mG in order to keep field-induced vortices from dominating the resistive transition and current-voltage characteristics near T_c . However, for thermoelectric measurements, a small external field of about 50 mG, supplied by a small superconducting solenoid, was used to smooth out resistance variations created by the temperature gradient. The "background" of field-induced vortices increased the uniformity of the current flow in the samples but did not perturb the thermoelectric measurements.

Each sample was characterized electrically by its resistive transition and current-voltage characteristics, as well as its thermoelectric response. Figure 2 shows representative data for sample 4. At higher temperatures, the resistance exhibits a fluctuation-broadened transition,⁸ while at lower temperatures it vanishes

with the exponential variation of a typical Kosterlitz-Thouless system.^{9,10}

The figure also shows the exponent $a(T)$ of the current-voltage characteristics, defined by $V = I a(T)$, where I is typically 0.1–1000 μA . This exponent displays an apparent "universal jump," rising nearly discontinuously from $a = 1$ to $a = 3$ as T is decreased to T_c from above, and increasing to larger values as T is lowered below T_c . In analyzing our data, we have adopted the convention that T_c is the temperature at which $a(T) = 3$. Following Fiory, Hebard, and Glaberson,¹¹ we deduce T_{c0} for our samples by fitting the resistive transition by the Aslamasov-Larkin^{8,9,11} expression for the temperature-dependent resistivity. Note from the figure that T_{c0} ($= 3.298$ K) derived in this way agrees well with the temperature ($= 3.302$ K) obtained by extrapolating $a(T)$ to unity.

The magnetic response of sample 4 to thermoelectric fields is also shown in Fig. 2 for typical values of I and ΔT . These data were obtained by measuring the magnetic flux $\Phi(T)$ at constant I , both with and without a temperature difference ΔT across the sample. The $\Delta T = 0$ data were subtracted to remove the residual background flux, and precautions were taken to verify that the signal did not originate from heaters, current-carrying wires, or other spurious sources. The magnetic flux rises rapidly above T_c to a maximum of about $10 \Phi_0$ between T_c and T_{c0} and then decays toward zero as the temperature approaches T_{c0} .

Figure 3 shows the magnitude of the thermoelectrically induced magnetization for four In/InO_x samples

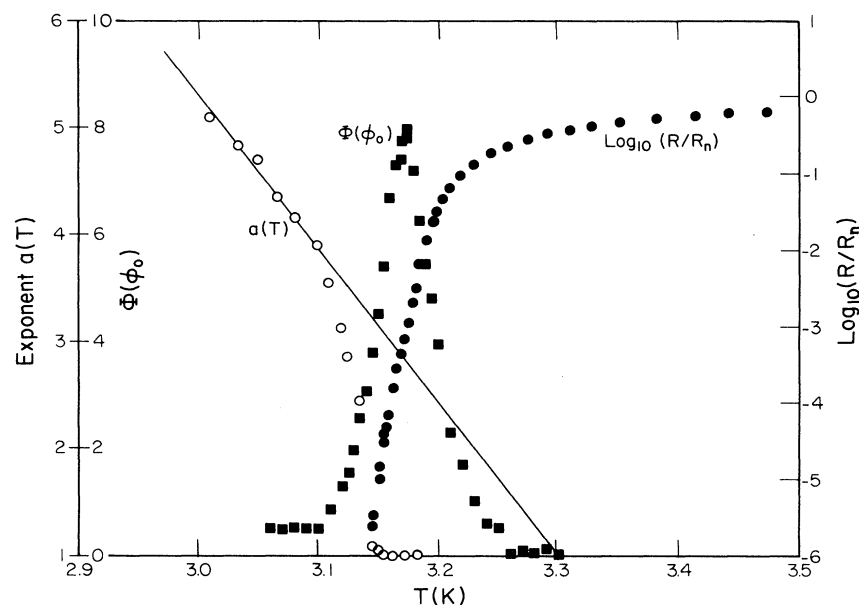


FIG. 2. The temperature dependence of the electrical resistance (closed circles), the exponent of current-voltage characteristics $a(T)$ (open circles), and the thermoelectrically induced flux Φ (squares) for sample 4. The resistance data were taken with a current of 0.25 μA , and the flux data with a current of 2.5 μA and a temperature difference of 10 mK.

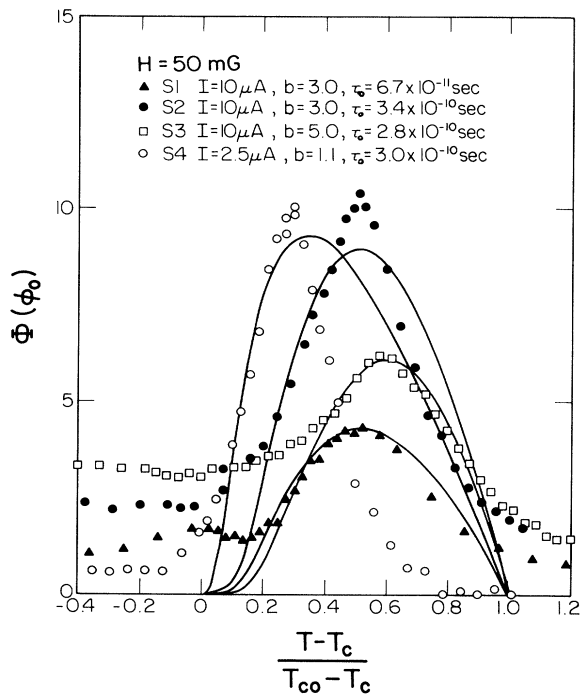


FIG. 3. The thermoelectrically induced flux for samples 1-4 as a function of reduced temperature. The data were taken at a current of 10 μA (2.5 μA for sample 4), and a reduced temperature difference of 0.070.

as a function of the reduced temperature $t = (T - T_c) / (T_{c0} - T_c)$, at a current $I = 10 \mu\text{A}$ (2.5 μA for sample 4), and a reduced temperature difference $\Delta t = \Delta T / (T_{c0} - T_c) = 0.070$. The data for all samples have similar general features, although the temperature of the magnetization peak, as well as its magnitude, varies from sample to sample.

In Fig. 4(a), we plot the magnetic response of sample 4 as a function of ΔT for four values of current I . The sample temperature (i.e., the value at the midpoint of the film) was maintained at 3.160 K, which is slightly below the location of the magnetization peak. The data show linear behavior, except for values of $\Delta T > 12 \text{ mK}$; for large temperature gradients, ΔT is a substantial fraction of $T_{c0} - T_c$ and nonlinear effects are to be expected. Figure 4(b) illustrates the variation of magnetic flux with sample current I for four values of ΔT . The magnetic flux is linear in the current (or, alternately, the electric field).

According to the GV model,⁶ a temperature gradient and electric field in a thin superconducting film upset the symmetrical balance of the thermally excited free-vortex-antivortex densities, leading to a dc magnetic field normal to the plane of the film. The thermoelectric fields drive the density of free vortices of each polarity out of local equilibrium, giving rise to a uniform

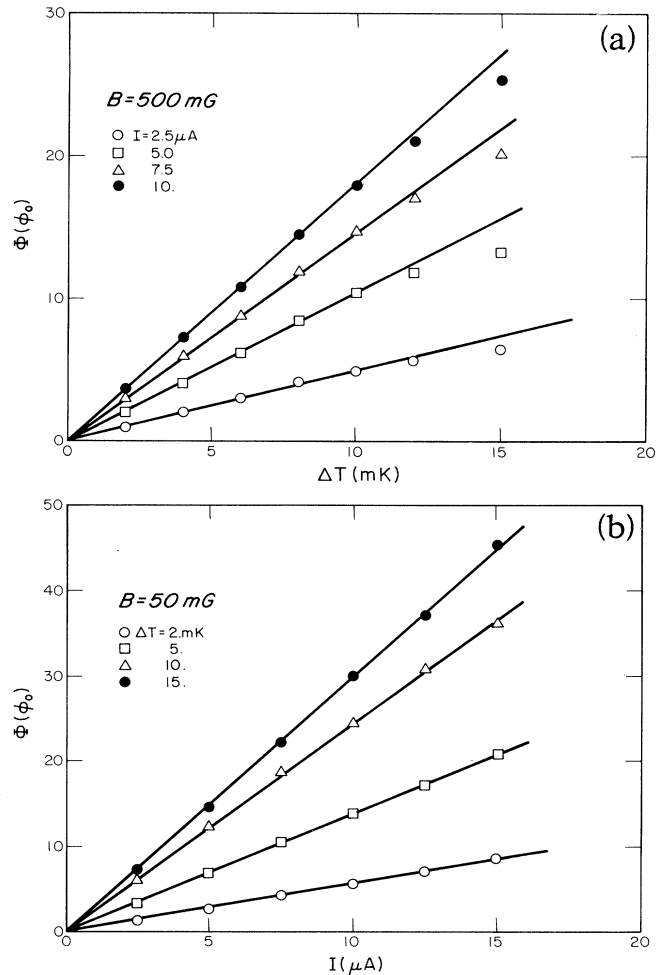


FIG. 4. The dependence of the thermoelectrically induced flux on (a) temperature difference at fixed sample current, and (b) sample current at fixed temperature different. Data are shown for sample 4 at a temperature of 3.160 K.

magnetization,

$$B = \Phi_0 (\delta n_{f+} - \delta n_{f-}). \tag{1}$$

In the above expression, $\Phi_0 = hc/2e$, and δn_{f+} and δn_{f-} are, respectively, the out-of-balance areal distribution functions for the vortices and antivortices. Assuming steady-state conditions, GV show that Eq. (1) can be expressed to lowest order in ∇T as

$$\mathbf{B} = \tau_0 [\partial \ln(n_{f0}) / \partial T] (\mathbf{E} \times \nabla T), \tag{2}$$

where τ_0 is a phenomenological time constant characterizing vortex relaxation, and n_{f0} is the equilibrium free-vortex density. This expression is expected to be valid for T near T_c .

The temperature dependence of \mathbf{B} predicted by Eq. (2) depends not only on the variation of the free-vortex density n_{f0} , but on the assumed time constant

τ_0 as well. In addition, because our measurement technique uses constant current injection, the electric field \mathbf{E} varies with temperature according to $\mathbf{E}(T) = \rho(T)\mathbf{J}$, where $\rho(T)$ is the vortex flux-flow resistivity and \mathbf{J} is the current density. The GV model predicts a magnetic flux that grows exponentially with temperature near T_c . The predicted behavior of \mathbf{B} at higher temperatures, however, depends on assumptions about the relaxation time τ_0 and the decay of the superfluid density near T_{c0} ; for a temperature-independent τ_0 , the predicted flux reaches a peak between T_c and T_{c0} and then decays to zero near T_{c0} with a $1 - (T/T_{c0})^4$ dependence.

The solid lines of Fig. 3 are fits of Eq. (2) to our data with b and τ_0 as temperature-independent fitting parameters. The data appear to agree with the general features of the model, including the rapid rise of the thermoelectric flux at T_c , the general appearance of a peak between T_c and T_{c0} , and the linear dependence of the flux on \mathbf{E} and ∇T . There are several other features of the data that are unexplained, however. The GV model predicts a broad asymmetrical peak, which contrasts with the resonancelike appearance of our data. Furthermore, the reasons for the sizable sample-to-sample variations of the magnitude of the flux, as well as the variations in the temperature of the flux peak are unknown. Neither of these quantities appears to be correlated with film resistivity or other obvious sample parameters.

In summary, we have observed directly the magnetic flux from thermally activated free vortices in thin superconducting films by driving the vortices out of equilibrium with thermoelectric fields. This thermoelectric effect appears to provide a useful way of

probing nonequilibrium vortex dynamics as well as the equilibrium vortex state.

This research was supported by the National Science Foundation Low Temperature Physics Program through Grant No. DMR-8106121. The facilities of the Ohio State University Materials Research Laboratory, Grant No. DMR-8119368, were used to prepare samples. The authors are grateful to T. R. Lemberger and D. J. VanHarlingen for numerous discussions, and to A. F. Hebard for valuable information on In/InO_x composite films.

¹J. M. Kosterlitz and D. J. Thouless, *J. Phys. C* **6**, 1181 (1973).

²M. R. Beasley, J. E. Mooij, and T. P. Orlando, *Phys. Rev. Lett.* **42**, 1165 (1979).

³B. I. Halperin and D. R. Nelson, *J. Low Temp. Phys.* **36**, 599 (1979).

⁴S. Doniach and B. A. Huberman, *Phys. Rev. Lett.* **42**, 1169 (1979).

⁵P. Minnhagen, *Phys. Rev. B* **23**, 5745 (1981).

⁶J. C. Garland and D. J. VanHarlingen, preceding Letter [*Phys. Rev. Lett.* **55**, xxx (1985)].

⁷A. F. Hebard and S. Nakahara, *Appl. Phys. Lett.* **41**, 12 (1982).

⁸L. G. Aslamasov and A. I. Larkin, *Phys. Lett.* **26A**, 238 (1968).

⁹A. F. Hebard and A. T. Fiory, *Phys. Rev. Lett.* **50**, 1603 (1983).

¹⁰A. M. Kadin, K. Epstein, and A. M. Goldman, *Phys. Rev. B* **27**, 6691 (1983).

¹¹A. T. Fiory, A. F. Hebard, and W. I. Glaberson, *Phys. Rev. B* **28**, 5075 (1983).